Functional Materials 13, No.2 (2006)

Phase formation and crystallization of films deposited by pulse laser sputtering of chromium in oxygen atmosphere

A.G.Bagmut, S.N.Grigorov, V.A.Zhuchkov, V.Yu.Kolosov*, V.M.Kosevich, G.P.Nikolaichuk

National Technical University "Kharkov Polytechnical Institute",
21 Frunze St., 61002 Kharkiv, Ukraine
*Ural State Economic University,
62 8th March St., 620026 Ekaterinburg, Russia

Received September 1, 2005

Effects of the substrate temperature T_S (20–420°C) and the oxygen pressure in the evaporation chamber $P(O_2)$ (10^{-5}–10^{-2} Torr) on the structure and phase composition of films obtained by pulse laser sputtering of a chromium target have been studied by electron microscopy (using the extinction bending contour technique to analyze the crystal lattice bending). At a fixed T_S, the oxygen content in amorphous films increases with increasing $P(O_2)$, while at a fixed $P(O_2)$, it decreases with elevating T_S. The influence of amorphous matrix composition and thickness t on the structure and morphology of crystals growing under annealing of the films by an electron beam has been studied. The bending of spherulite crystal lattice has been found to decrease with increasing overstoichiometric Cr concentration in amorphous matrix and with increasing distance up to the center of an zone-axial pattern of the spherulite. At small film thickness $t \le t^* \approx 2.5$ to 3 nm, the crystallization is hindered due to dimensional and impurity effect of the amorphous state stabilization.

Проведено электронно-микроскопическое исследование (с использованием техники анализа искривления кристаллической решетки методом изгибных экстинкционных контуров) влияния температуры подложки T_S (20–420°C) и давления кислорода в испарительной камере $P(O_2)$ (10^{-5}–10^{-2} торр) на структуру и фазовый состав пленок, полученных лазерным распылением мишени хрома. При фиксированной T_S содержание кислорода в аморфных пленках возрастает с увеличением $P(O_2)$, а при фиксированном $P(O_2)$ – уменьшается с ростом T_S. Изучено влияние состава и толщины t аморфной матрицы на структуру и морфологию кристаллов, растущих при отжиге пленок электронным лучом. Показано, что искривление кристаллической решетки сферолитов уменьшается с увеличением концентрации в аморфной матрице избыточного сверхстехиометрического хрома и с увеличением расстояния до центра зонно-осевой картины сферолита. При $t \le t^* \approx 2{,}5$–3 нм кристаллизация затруднена вследствие проявления размерно-примесного эффекта стабилизации аморфного состояния.

The parameters defining the structural and phase state of a thin-film condensate at laser sputtering of metal targets, include the density of vapor-plasma flow of sputtered metal and the presence of high-energy microparticles therein; the flow density of residual gas particles in the evaporation chamber; the ability of metal to adsorb gas impurities and to form chemical compounds therewith; the substrate type, orientation, and temperature. For the case of metal condensation on a substrate at room temperature, a diagram has been constructed reflecting the film structural condition de-

pending on the ration of gas (oxygen) and metal atomic flows hitting the surface of a growing film as well as on the metal adsorption and chemical activity [1]. It is shown that as the relative fraction of the metal component in the flow is decreased, the following structures are consecutively realized in laser condensates of Cr: crystal metal; films with amorphous component at metal grain boundaries; amorphous conglomerate structures; and oxygenated phases with a composition close to the stoichiometric oxide.

The structural and morphological crystallization features of amorphous films prepared by laser sputtering of chromium followed by condensation of the erosion products on substrates at room temperature have been investigated in [2, 3]. It was established that annealing of amorphous oxygen-containing chromium laser condensates of a composition close to the stoichiometric one composition (Cr_2O_3) causes a polymorphic crystallization (without changing of the chemical composition). The relative density average increasing at crystallization of amorphous Cr_2O_3 films is about 7.2 %. During the Cr_2O_3 crystal nucleus growth, a complex trans-rotational distortion of the crystal lattice takes place, which is inherent in the spherulite formation process at an amorphous film crystallization [4, 5]. At the trans-rotational distortion, the crystal lattice is formed with a continuous monotonous bending (up to 120 degree per micrometer) about an axis lying in the film plane. The crystal itself remains flat [5]. The integrated and local bends of crystal lattices for Cr_2O_3 spherulites of various configurations have been determined in [2, 3].

The aim of this work is (i) to study the influence of the substrate temperature T_S and the oxygen pressure $P(O_2)$ in the evaporation chamber on the structure and phase composition of chromium laser condensates by electron microscopy; (ii) to study the influence of the film thickness t and the amorphous matrix composition on the structure and morphology of crystals growing during annealing of amorphous films with electron beam.

The targets of high purity chromium where sputtered using the emission pulses of an AlG:Nd^{3+} laser (1.06 μm wavelength) operating in the Q-switch mode. The pulse repetition frequency $\nu = 25$ Hz. The products of laser erosion where condensed on orienting substrates cleaved out of KCl single crystals along the cleavage planes (001) and on neutral substrates of KCl single crystals covered with thin carbon film (transparent for an electron beam). The substrate temperature T_S was varied from 20 to 420°C. The evaporation chamber was initially evacuated down to a pressure $P \approx 10^{-5}$ Torr. Then oxygen was introduced up to required pressure using a SNA-2 bleeding system. The Cr target was sputtered in oxygen atmosphere at a pressure $P(O_2) \sim 10^{-5}$ to 10^{-2} Torr in a flow-through mode. The films were separated from the substrates in distilled water and then transferred onto object grids for electron microscopy. The phase transformation from amorphous to a crystalline state was initiated using local heating with electron beam in the microscope column (the "in situ" technique). The structures were analyzed by electron diffraction and transmission electron microscopy (EM-100L, TEM-125K) using the bent extinction contour technique [2–5]. Using the electron-microscopic images, the specific local rotation angle of the crystal lattice θ_{loc} (describing rotation of crystal planes per unit length of the crystal in °/μm) according to the relation:

$$\theta_{loc} = \frac{360}{\pi W} \arcsin\left(\frac{\lambda}{2d_{hkl}}\right), \qquad (1)$$

where W is the distance between a pair of bent extinction contours corresponding to diffraction vectors $\mathbf{g}_{hkl}$ and $\mathbf{g}_{\bar{h}\bar{k}\bar{l}}$; d_{hkl}, interplane spacing; λ, the electron wavelength.

The film thickness t was determined using a technique [4] from the relation

$$t = \frac{d_{hkl}^2 W}{\lambda \varepsilon}, \qquad (2)$$

where ε is the distance between interference images of a bent extinction contour in dark field (Fig. 1). For a case given in Fig. 1 ($d_{300} = 1.431$ Å; $\lambda = 0.037$ Å and $W/\varepsilon = 3.92$), it follows from (2) that $t \approx 217$ Å.

The thickness t influence on the film crystallization character was studied on films of variable thickness deposited using the "wedge" technique. A thin metal plate with smooth peaked edge masked the substrate surface, thus allowing to obtain a significant film thickness gradient (grad $t \sim$ 3–4 Å/μm). In this case, the film thickness was changed monotonously from zero up to the maximal value $t_{max} \approx 22$ nm within 1 or 2 cells of the electron microscope object grid.

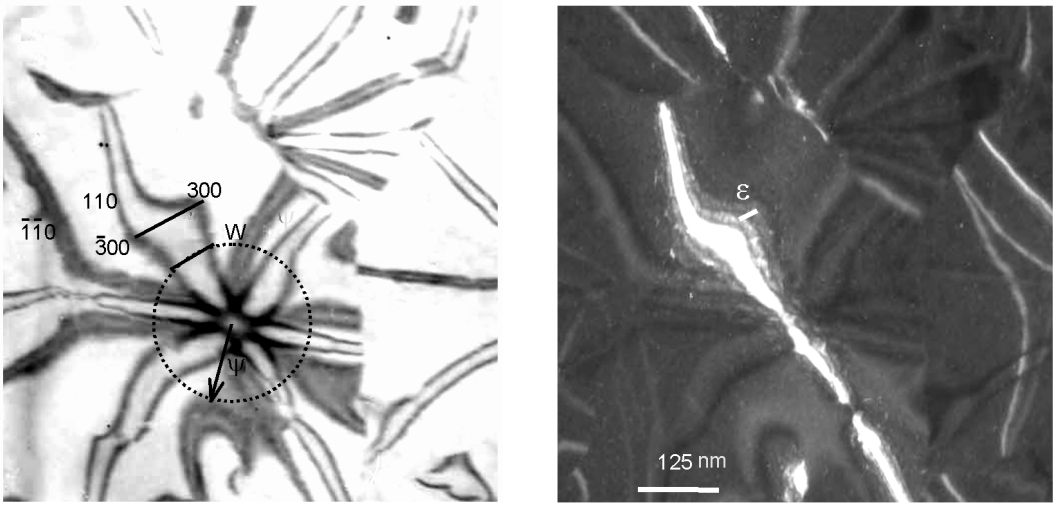

a b

Fig. 1. A scheme illustrating the determination of the film thickness t and the local rotation angle of crystal lattice planes θ_{loc}: (a) light field electron-microscopic image of a Cr_2O_3 spherulite (the zone axis oriented along [001]); (b) the same area in the reflection light of 300 Cr_2O_3.

Influence of gas environment and condensation temperature on structure and phase composition of chromium laser condensates. The substrate temperature T_S effect on the film structure formation was studied at a fixed oxygen pressure $P(O_2) = 10^{-3}$ Torr at temperature T_S varying from 20 to 420°C. The results obtained are illustrated by the data of Table 1. In a temperature interval $T_S = 20–150$°C, single-phase amorphous films with structure close to Cr_2O_3 oxide are formed. At $T_S = 200–300$°C, two-phase condensates are formed comprising finely dispersed Cr crystals and amorphous Cr_2O_3 (Fig. 2a). An enlarged dark-field image of Cr precipitate is presented in the left top corner of the microphotograph in Fig. 2b. The effect of epitaxy of chromium microparticles on KCl is clearly seen in orientation relation:

$$(001)\langle 110\rangle Cr \| (001)\langle 100\rangle KCl. \qquad (3)$$

The epitaxy effect is intensified as T_S increases. The content of chromium crystals in a film increases, too. At $T_S = 350–420$°C, two-phase crystalline condensates are formed containing finely dispersed Cr and Cr_2O_3 crystals (Figs. 2c and 3d). The orientation relation of Cr_2O_3 and Cr lattices takes place:

$$\langle 44\bar{1}\rangle Cr_2O_3 \| \langle 001\rangle Cr, \qquad (4)$$

where the (001) Cr_2O_3 planes are practically parallel to (101) Cr ones.

Table 1. Structure and phase composition of Cr laser condensates

T_S, °C	$P(O_2)$, Torr	Condensate structure and phase composition
20	10^{-5}	Amorphous Cr and Cr–O
	10^{-3}	Amorphous Cr_2O_3
	10^{-2}	Amorphous Cr_2O_3
100	10^{-3}	Amorphous Cr_2O_3
150	10^{-3}	Amorphous Cr_2O_3
200	10^{-3}	Amorphous Cr_2O_3 and Cr crystals
300	10^{-5}	Cr crystals
	10^{-3}	Amorphous Cr_2O_3 and Cr crystals
350	10^{-3}	Cr_2O_3 and Cr crystals
420	10^{-3}	Cr_2O_3 and Cr crystals

It is natural that on the heated-up KCl substrates the effect is revealed at the same relation (3) at chromium laser evaporation in vacuum ($P = 10^{-5}$ Torr). In the presence of amorphous carbon thin-film underlayer, no epitaxy effect is observed. The comparison of data presented in Table 1 indicates that at fixed $P(O_2)$, the oxygen capture efficiency by the growing film decreases with the increasing substrate temperature T_S.

Crystallization of films with amorphous component: internal bending of the spherulite crystal lattice. The crystallization morphological features of films including amorphous Cr_2O_3 component was investigated by "in situ" electron microscopy. To evaluate quantitatively the internal distor-

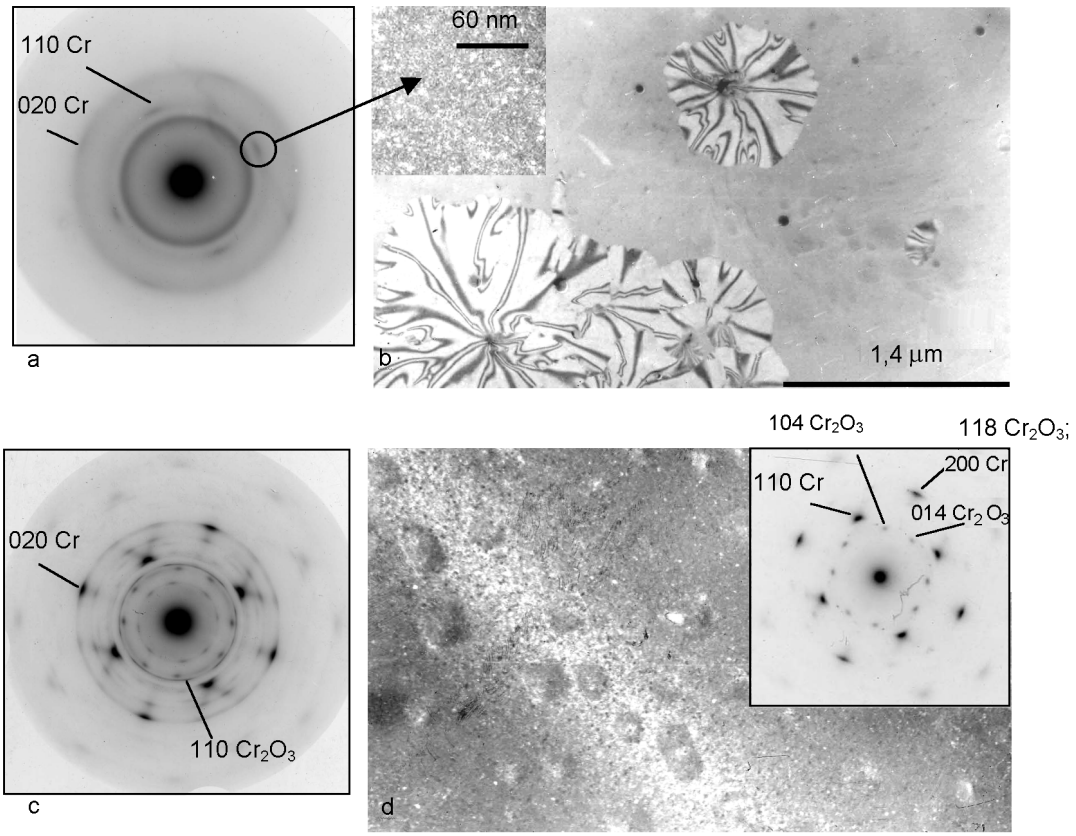

Fig. 2. Structure of Cr condensates laser-sputtered in oxygen at $P(O_2) = 10^{-3}$ Torr: (a) electron diffraction pattern of a film containing oriented crystalline Cr inclusions in an amorphous matrix (initial state, $T_S = 200$°C); (b) the same film after a partial crystallization under electron beam (in the upper top corner, the enlarged dark-field image of the film in the light of Cr $1\bar{1}0$ reflection); (c) electron diffraction pattern of a crystalline film ($T_S = 420$°C); (d) microphotograph of the same film (in the upper top corner, the microdiffraction pattern).

tion of Cr_2O_3 spherulite crystal lattice, microphotographs of crystals with distinct [001] zone-axial patterns of bent extinction contours (as in Fig. 1a) have been used. Only the pairs of bend contours corresponding to diffraction vectors $\mathbf{g}_{hkl}$ and $\mathbf{g}_{\bar{h}\bar{k}l}$ were taken into account for which triplets of *hkl* indices were 300, 030, and $\bar{3}30$.

At fixed pressure $P(O_2) = 10^{-3}$ Torr, the amorphous component was present in the films at condensation temperatures $T_S = 20$, 100, 150, 200, and 300°C (Table 1). The sample size for each T_S corresponded to 50–100 pairs of bent extinction contours. Since in (1) the distance W between pair of bent extinction contours corresponding to diffraction vectors $\mathbf{g}_{hkl}$ and $\mathbf{g}_{\bar{h}\bar{k}l}$ depends on the distance ψ up to the zone-axial pattern center, all measurements were carried out at the fixed ψ values of 0.075; 0.100; 0.125; 0.150 and 0.175 μm.

The statistical evaluation results of measurements performed using the relation (1) are presented in Fig. 3. There are the following regularities. (i). As the condensation temperature T_S increases, the specific local crystal lattice rotation angle θ_{loc} tends to increase (Fig. 3a). The amorphous low-temperature laser condensates are enriched in Cr and do not correspond to stoichiometric composition of Cr_2O_3. As the T_S increases, chromium precipitates as a separate crystal phase, and the composition of amorphous film component approaches the stoichiometric composition Cr_2O_3. Hence, it is to conclude that as the excess concentration of over-stoichiometric chromium in amorphous film increases, the θ_{loc} value decreases. (ii). The θ_{loc} decreases also with increasing distance ψ to the zone-axial pattern center (Fig. 3b).

Heterogeneous nucleation and conjunction of Cr_2O_3 crystals differing in orientation and morphology. It has been established before [2] that the crystals of three main morphological types are formed at the in-

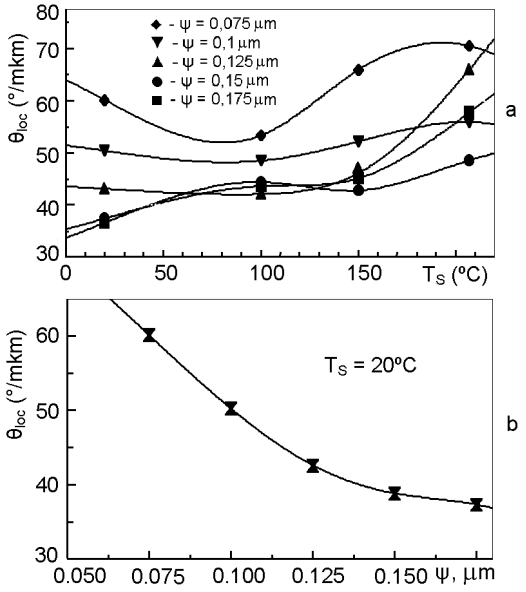

Fig. 3. Crystal lattice distortion of Cr_2O_3 spherulites growing in the amorphous component of laser-sputtered Cr condensates under the film heating by an electron beam: (a) θ_{loc} dependence on T_S; (b) θ_{loc} dependence on the distance ψ to the zone-axial pattern center.

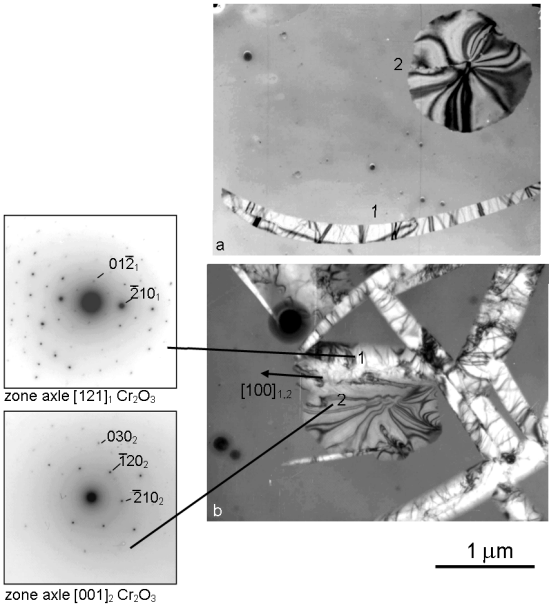

Fig. 4. (a) Two main morphologies of crystals growing at crystallization of amorphous Cr_2O_3 films, strip-like (*1*) and rounded (*2*); (b) oriented growth of a rounded crystal (*2*) at the lateral surface of the strip-like one (*1*).

itial transformation stage. The rounded shape crystals are oriented with the basic plane (001) parallel to the film surface. The strip-like crystals and crescent-shaped ones may be oriented with various planes parallel to the film surface.

In this work, it has been found that as a rule, the homogeneous nucleation of strip-like crystals takes place in amorphous matrix (the terminology used in [2] is kept). The crescent-shaped crystals are formed during the trans-rotational distortion of the strip-like ones. The rounded shape crystals can nucleate in the free state (Fig. 4a), as well as in a bound state, heterogeneously at the lateral surface of strip-like crystals. Fig. 4b illustrated the latter case. Under heating of the film with electronic beam, the strip-like crystal 1 homogeneously nucleates and grows in amorphous matrix. An interpretation of a selected diffraction pattern (zone axis is [121]) has shown that the (015) Cr_2O_3 planes are oriented parallel to the film surface and the strip-like crystal long axis is directed along [100] (Table 2, line 1). The nucleation and growth of a rounded shape crystal 2 occurs heterogeneously at the lateral surface of the crystal 1 perpendicular to the film surfaces and parallel to $(01\bar{2})$ of Cr_2O_3. The relation $(015)_1[10\ 0]_1 // (0\ 01)_2[1\ 0\ 0]_2$ is carried out. The lattices of crystals 1 and 2 are rotated with respect to one another at the angle $\beta = 32.3°$ about the common axis [100]

Table 2. Main conjugation types of two Cr_2O_3 crystals having two main morphologies

No.	Crystal morphology					Orientation relation	Rotation axis	Rotation angle β, degree	Conjugated planes (perpendicular to the film plane)
	Strip-like			Rounded					
	$[uvw]_{\uparrow}$	$(hkl)_{\parallel}$	$[uvw]_{\leftrightarrow}$	$[uvw]_{\uparrow}$	$(hkl)_{\parallel}$				
1	[121]	(015)	[100]	[001]	(001)	$(015)_I\ [100]_I \parallel (001)_2\ [100]_2$	$[100]_{1,2}$	32.3	$(01\bar{2})_1 \mid (010)_2$
2	[$\bar{1}$10]	($\bar{1}$10)	[110]	[001]	(001)	$(\bar{1}10)_1\ [110]_1 \parallel (001)_2\ [110]_2$	$[110]_{1,2}$	90	$(011)_1 \mid (\bar{1}10)_2$
3	[$\bar{6}$61]	($\bar{6}$65)	[1 $\bar{1}$ 12]	[001]	(001)	$(\bar{6}65)_1\ [1\ \bar{1}\ 12]_1 \parallel (001)_2\ [\bar{2}10]_2$	$[1\ \bar{1}\ 12]_1$	75.2	$(110)_1 \mid (010)_2$
4	[001]	(001)	[110]	[001]	(001)	$(001)_1\ [110]_1 \parallel (001)_2\ [110]_2$	$[100]_{1,2}$	0;180	$(\bar{1}10)_1 \mid (\bar{1}10)_2$

Remark: $[uvw]_{\uparrow}$ the zone axis indices; $(hkl)_{\parallel}$, indices of the crystal plane parallel to the film surface: $[uvw]_{\leftrightarrow}$, indices of direction parallel to the long axis of the needle-like crystal.

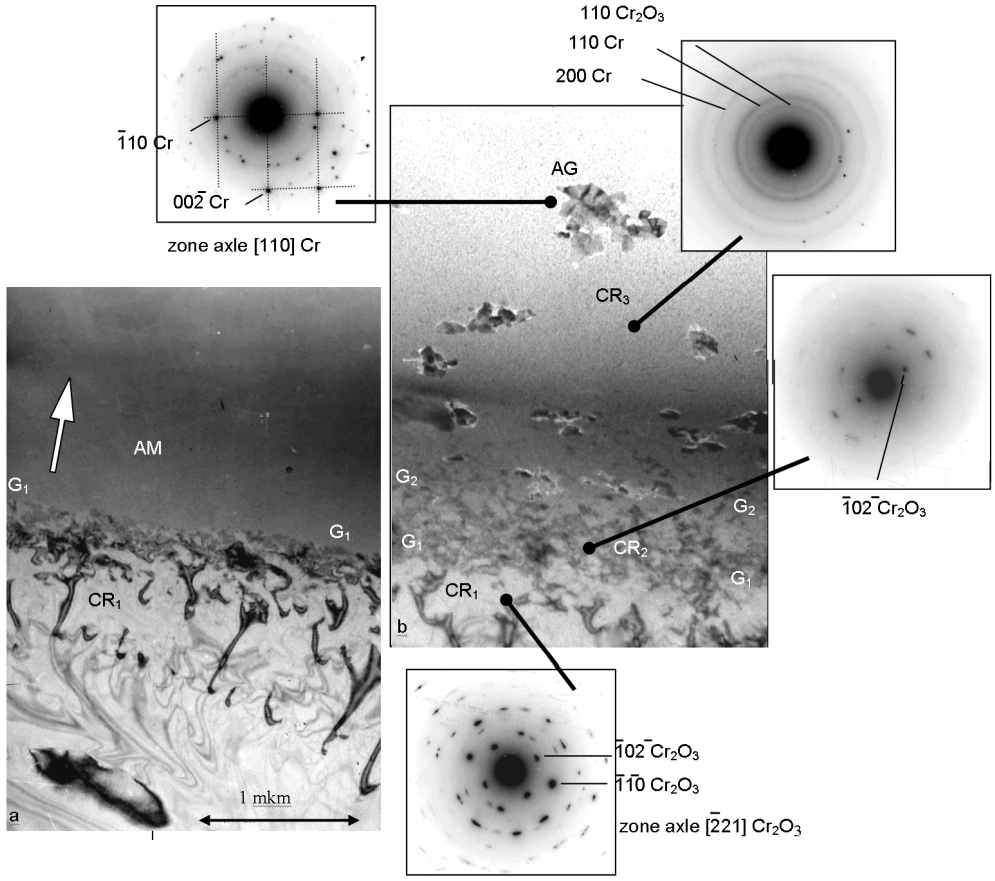

Fig. 5. Consecutive crystallization steps of a variable thickness amorphous layer. The crystallization front (CF) movement direction (towards the reducing thickness) is shown by an arrow: (a) line G_1–G_1 corresponding to the CF stop at $t < t^*$ (2.5 to 3 nm); (b) the further CF moving (to the G_2–G_2 position) at a significantly increased heating intensity.

(β is the angle between axes of [121] and [001] zones).

The study results for the most characteristic conjunction types of Cr_2O_3 crystals of various morphologies are shown in Table 2. Data of that Table as well as the direct electron-microscopic observations evidence that at final stages, the crystal phase is formed mainly by rounded shape crystals. In this case, the crystal/vacuum interface has the minimal energy, since it is presented with (0 0 1) Cr_2O_3 planes with the least Miller indices.

Crystallization at variable amorphous layer thickness. Fig. 5 presents an area of a film with variable thickness t deposited by laser sputtering of chromium in oxygen atmosphere ($P(O_2) = 10^{-3}$ Torr, $T_S = 20°C$) in conditions of partial substrate surface screening against the vapor-plasma flow. At the film heating by an electron beam (at a fixed beam current density) moving in the direction of the film thickness reduction, the crystallization front was moved in the same direction at a constant speed $V \sim 1$ μm/s. The following effects were observed.

(i) The film crystallization stops when its thickness becomes less than critical value $t^* \approx 2.5$–3 nm. In Fig. 5, the line G_1–G_1 corresponding to the first stop of the film crystallization front is clearly visible. It divides the crystalline (CR_1) and amorphous (AM) film areas. The area CR_1 is filled with a crystalline Cr_2O_3 phase which is oriented so that zone axis [$\bar{2}21$] is perpendicular to the film plane. Thus, the plane ($\bar{2}25$) Cr_2O_3 is oriented in parallel to the film plane. A similar effect is observed also at other orientations of Cr_2O_3 crystals in the CR_1 area, in particular, when the (001) Cr_2O_3 plane is parallel to the film plane.

(ii) The increasing heating intensity initiates an insignificant movement of the crystallization front in the direction of t reduction up to the G_2–G_2 line corresponding to the second stop of the crystallization front (Fig. 5b). The area CR_2 between G_1–G_1 and G_2–G_2 lines is filled with the

crystalline Cr_2O_3 phase having the same orientation as the CR_1. It is followed by area CR_3 enriched in chromium and represented by finely dispersed crystalline phases of Cr_2O_3 and Cr. The further film heating initiates the sintering of chromium microcrystals and formation of agglomerates (AG), where the sizes of Cr crystals in the film plane may reach ~ 0.5 μm (Fig. 5b). For clariness sake, in the selected area of diffraction pattern from the AG area, the reflections from planes belonging to the [110] Cr zone are joined by a network of lines.

It has been noted [6] that the existence areas of amorphous phases are limited in the film thickness t and in temperature T and become extended noticeably in these parameters at introduction of impurities. The dimensional effect is manifested itself as the amorphous phase stabilization with reduction of the film thickness. Before, it was established [7] taking amorphous Sb films as an example that as the thickness reduces, the characteristic kinetic time of crystallization increases. At a fixed environmental temperature, the amorphous state can be kept infinitely, if the film thickness is less than critical value t^* (in the case of Sb at room temperature, $t^* \approx 10$ nm). According to [6], a probable reason for the increase of the amorphous-to-crystal transition temperature with reduction of t (at positive transition heat) may consist in increasing surface energy at film crystallization. Besides, the crystallization is connected with the overcoming of an activation barrier separating the amorphous and crystal states, its height raising as t reduces.

The presence of impurity in the film stabilizes also the amorphous state. Widespread is the opinion that the impurity atoms induce formation of various types interatomic bonds, that results in disruption of coordination identical ver the whole volume [6]. The occurrence of a disordered structure with mixed bonds appears to be more favorable thermodynamically than the formation of close packing with equal and identical bonds.

The experimental data from this work, where the film structure changes with changing thickness, can be considered as a manifestation of dimensional/impurity effect of amorphous state stabilization. If the film thickness gradient was created intentionally, the enrichment of a thin layer adjacent to substrate in chromium was spontaneous. The latter may be due to the following factors: (a) variation of oxygen adsorption ability of the surface during the substrate filling by products of the target laser sputtering; (b) displacement of impurity chromium atoms at the crystallization front from the crystal matrix into amorphous one; (c) deviation of the oxygen and chromium atomic flow ratio towards the increasing at the flow scattering at the edge of the metal plate screening the vapor-plasma flow. To determine the influence extent of each of the listed factors requires a further experimental research.

To conclude, amorphous films enriched in chromium are crystallized under heating with release of Cr and Cr_2O_3 crystals. Amorphous films of the stoichiometric composition are crystallized forming Cr_2O_3 crystals only. At a fixed oxygen pressure in the evaporation chamber, the oxygen capture efficiency of a film growing from laser erosion plasma of chromium decreases as the substrate temperature rises. In the substrate temperature range from 350 up to 420°C, two-phase crystalline condensates of Cr and Cr_2O_3 are formed with the orientational connection of crystal lattices meeting the relation $<44\bar{1}>$ Cr_2O_3 $\|$ <001> Cr. At the crystallization of the amorphous film component induced by an electron beam heating, the θ_{loc} angle characterizing the bending of spherulite crystal lattice decreases with the increasing concentration of excessive over-stoichiometric chromium. As well as with increasing distance ψ to the center of a zone axial pattern. In most cases, homogeneous nucleation of arbitrarily oriented strip-like Cr_2O_3 crystals appear in amorphous matrix at the crystallization. The crescent-like crystals are formed in the course of trans-rotational distortion of strip-like crystals. The rounded shape crystals are nucleated heterogeneously at the lateral surface of strip-like and crescent-like crystals of Cr_2O_3. When the film thickness $t \le t^* \approx 2.5-3$ nm, the film crystallization is hindered due to a dimensional/impurity effect of amorphous state stabilization.

This work has been supported financially by INTAS (Grant №.00-100).

References

1. A.G.Bagmut, V.M.Kosevich, G.P.Nikolaichuk, *Functional Materials*, **6**, 75 (1999).
2. A.G.Bagmut, S.N.Grigorov, V.Yu.Kolosov et al., *Functional Materials*, **10**, 687 (2003).
3. V.Yu.Kolosov, K.L.Shvamm, A.G.Bagmut, S.N.Grigorov, *Poverkhnost'*, 10, 100 (2004).
4. V.Yu.Kolosov, A.R.Tholen, *Acta Materialia*, **48**, 1829 (2000).

5. V.Yu.Kolosov, L.M.Veretennikov, *Poverkhnost'*, **2**, 70 (2000).
6. Yu.F.Komnik, *Fiz.Nizk.Temper.*, **8**, 3 (1982).
7. L.S.Palatnik, M.Ya.Fuks, V.M.Kosevich, Formation Mechanism and Substructure of Condensed Films, Nauka, Moscow (1972) [in Russian].
8. A.G.Bagmut, S.N.Grigorov, V.Yu.Kolosov et al., *Poverkhnost'*, No.10, 60 (2003).

Фазоутворення і кристалізація плівок, осаджених імпульсним лазерним розпиленням хрому в атмосфері кисню

О.Г.Багмут, С.М.Григоров, В.А.Жучков, В.Ю.Колосов, В.М.Косевич, Г.П.Николайчук

Проведено електронно-мікроскопічне дослідження (із використанням техніки аналізу скривлення кристалічних граток методом згинних екстинкційних контурів) впливу температури підкладки T_S (20–420°C) і тиску кисню у випарній камері $P(O_2)$ (10^{-5}–10^{-2} торр) на структуру і фазовий склад плівок, осаджених лазерним розпиленням мішені хрому. При фіксованій T_S вміст кисню в аморфних плівках зростає зі збільшенням $P(O_2)$), а при фіксованому $P(O_2)$ – зменшується з ростом T_S. Вивчено вплив складу і товщини t аморфної матриці на структуру і морфологію кристалів, що ростуть при відпалі плівок електронним променем. Показано, що скривлення кристалічних граток сферолітів зменшуються зі збільшенням концентрації в аморфній матриці надлишкового надстехіометричного хрому і зі збільшенням відстані до центра зонно-осьової картини сфероліту. При $t \le t^* \approx 2.5$–3 нм кристалізація утруднена внаслідок прояву розмірно-домішкового ефекту стабілізації аморфного стану.